Oscillatory instability of deep cells in directional solidification

Alain Karma
Department of Physics, Northeastern University, Boston, Massachusetts 02115

Pierre Pelcé
Laboratoire de Recherche en Combustion, Université de Provence–St. Jerome, 13397 Marseille CEDEX 13, France
(Received 9 August 1988)

Coherent sidebranching of deep cells has been observed experimentally in the vicinity of the cell to dendrite transition. We propose that this phenomenon results from an oscillatory instability of deep cells, where cell widths and tip positions oscillate coherently in phase. We perform a linear-stability analysis of a periodic array of deep cells in the small-Péclet-number limit and derive the stability limits of the oscillatory mode.

I. INTRODUCTION

The experimental data of Dougherty, Kaplan, and Gollub[1] support recent theories which have advanced that sidebranching on the sides of an unconstrained isolated dendrite growing in an infinite medium is the result of the amplification of noise at the tip of the dendrite (Langer and co-workers,[2–4] Pelcé and Clavin.[5]) In particular, their measurements have indicated that there is no apparent temporal correlations between sidebranching events on opposite sides of the dendrite at some fixed distance behind the tip.

Sidebranching also occurs during the directional solidification of a binary liquid mixture at sufficient growth velocity. However, in this system, the experimental photographs of Eshelman, Seetharaman, and Trivedi[6] suggest that, at least in some cases, sidebranching events on neighboring cells are correlated. This behavior can be seen most clearly in the vicinity of the cell to dendrite transition where sidebranches first appear on the sides of very-large-amplitude cells [in the pivalic acid–ethanol system this transition occurs for drawing velocities around 5–7 μm/s for a temperature gradient $G=2.98$ K/mm (Ref. 6)]. This type of "coherent sidebranching" extends spatially over several cells and is marked on the experimental photographs by the appearance of equally spaced strips parallel to the solidification front. At this point a more detailed quantitative experimental study of this phenomenon is needed before reaching any firm conclusions. Nevertheless, it suggests the possibility that in directional solidification a completely different dynamical mechanism can be responsible for sidebranching in certain parameter ranges.

In this paper, we demonstrate that, in the small-Peclet-number limit, a periodic array of deep cells undergoes an oscillatory instability at sufficiently large growth velocity. Above the threshold of this instability the width and the vertical tip position of all cells oscillate in phase coherently as depicted schematically in Fig. 1. We propose that the coherent sidebranching which has been observed experimentally results from this instability.

Our theoretical analysis is made possible by the fact that, in the small-Peclet-number limit, the full free-boundary problem can be considerably simplified and reduced essentially to a one-dimensional problem where the slow dynamical evolution of the tip region of the cells is represented by the motion of a point source in a semi-infinite medium. This reduction relies solely on the assumption that the tail region of deep cells adjusts to the motion of the tip region without affecting it.

This paper is organized as follows. In Sec. II we derive the equations of motion for the cell tips in the small-Peclet-number limit. In Sec. III we then derive a relationship between tip undercooling and cell spacing for the one-parameter family of steady-state solutions of the equations of motion. In Sec. IV we perform a linear-stability analysis of the steady-state solutions and derive the stability limits for the oscillatory mode. Finally in Sec. V we discuss the physical relevance of our result.

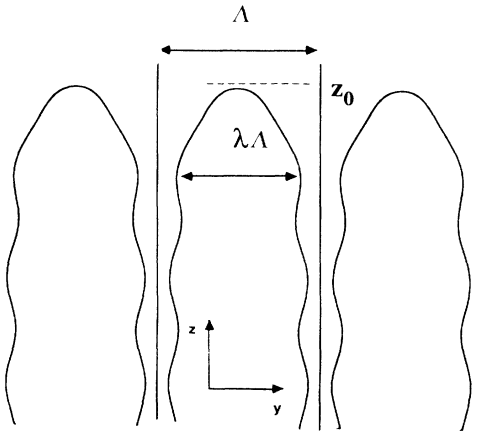

FIG. 1. Schematic diagram exhibiting coherent sidebranching of deep cells. $\lambda\Lambda$ and λ are the cell spacing and the cell width, respectively, and z_0 is the cell-tip position.

II. EQUATIONS OF MOTION

A. The free-boundary problem

In directional solidification of a binary liquid mixture, the motion of the solidification front is determined by the diffusion of solute in the melt together with a set of boundary conditions on the interface. A more introductory and detailed exposition of the directional solidification system can be found in Ref. 7. We only summarize here the basic equations governing interface motion and our notation. The solute concentration c satisfies the usual diffusion equation,

$$\frac{\partial c}{\partial t}=D\,\Delta c\ , \tag{1}$$

in the liquid, and diffusion in the solid is neglected. Temperature and solute concentration at the interface are related to the local interfacial curvature by the Gibbs-Thomson relation,

$$T=T_0+mc-\frac{\sigma T_0}{QR}\ . \tag{2}$$

Here, D is the coefficient of solute diffusivity in the liquid, m the slope of the liquidus line in the binary phase diagram, T_0 the crystallization temperature of the pure melt, R the local radius of curvature, Q the latent heat released per unit volume, and σ the liquid-solid surface tension. In the slow-growth regime the latent heat release at the interface can be neglected. Consequently, the temperature in the sample is simply $T=T_p+Gz$, where $T_p=T_0+mc_\infty/K$ is the temperature of the planar interface, G the temperature gradient imposed on the sample, K the partition coefficient, and c_∞ the bulk mixture composition.

In addition, solute conservation at the interface requires

$$c(1-K)\mathbf{v}\cdot\mathbf{n}=-D\,\nabla c\cdot\mathbf{n}\ . \tag{3}$$

We want to describe the dynamics of a periodic array of cells of primary spacing Λ. We therefore restrict the sample to a region of liquid of width Λ, with on the sides of this region ($y=\pm\Lambda/2$, where y is the transverse coordinate) the additional boundary condition $\partial c/\partial y=0$.

B. Scalings and regions in the small-Peclet-number limit

As shown previously by Pelcé and Pumir,[8] and Karma,[9] this free-boundary problem can be simplified in the small-Peclet-number (P) limit, where $P=\Lambda U/D$, and U is the velocity of the interface. Three regions can be distinguished.

1. The diffusion region

In the liquid, far away from the interface, the concentration field can be considered monodimensional, as in the case of the planar interface. The concentration field varies on a lengthscale $l=2D/U$ and satisfies the monodimensional diffusion equation, i.e.,

$$\frac{\partial c}{\partial t}=D\frac{d^2c}{dz^2}\ . \tag{4}$$

The relative variation of concentration on a scale l in the liquid is of order unity.

2. The tip region

Close to the tip of the cell, the concentration field varies on a scale Λ, very small compared to the diffusive length l. As a result, the Laplacian term dominates in Eq. (1) and the diffusion equation reduces to $\Delta c=0$.

Local interfacial deformations on a scale of order Λ relax on a time scale Λ^2/D which is very small compared to the diffusive time scale D/U^2. Consequently, the tip region can be assumed to remain quasistationary during the motion of cell tips with velocity $U(t)$ on the slow diffusive time scale.

The relative magnitude of concentration variations in this region, $\delta c/c_\infty$, is of order P. The concentration flux which leaves the tip region, $-D\,\delta c/\Lambda$, equals the flux which enters the diffusion region, Uc_∞. Thus, $\delta c/c_\infty\approx P$ and c can be approximated by the constant

$$c_0=c_\infty/K+z_0(G/m) \tag{5}$$

in Eq. (3), where z_0 is the position of the cell tip. Since the capillary length is small compared to the cell spacing, the contribution of the surface-tension term of order P and thus does not appear in Eq. (5).

For convenience, one defines a new field $\Phi=c-c_\infty/K-zG/m$ which still satisfies

$$\Delta\Phi=0 \tag{6}$$

with the corresponding boundary conditions on the interface:

$$\phi=-d_0c_L/R\ , \tag{7}$$

which can be deduced from Eq. (2) and

$$-D\,\nabla\Phi\cdot\mathbf{n}=[c_0(1-K)U+G(D/m)]\cos\theta \tag{8}$$

from Eq. (3). Here, $d_0=\sigma T_0/|m|Q$ is the capillary length.

On the sides of the sample ($y=\pm\Lambda/2$) the boundary condition $\partial\Phi/\partial y=0$ still holds. Far ahead of the cell, in the region $\Lambda\ll(z-z_0)\ll1$, the concentration flux becomes uniform and thus $d\Phi/dz$ is equal to

$$\frac{d\Phi}{dz}=-\lambda\left[c_0(1-K)\frac{U}{D}+\frac{G}{m}\right]\ . \tag{9}$$

The free-boundary problem defined by Eq. (6) and boundary conditions (7) and (8) is formally identical to the Saffman-Taylor free-boundary problem, which determines the motion of a viscous finger in a Hele-Shaw cell. The field Φ is the analog of the pressure field in the Saffman-Taylor problem and the linear temperature gradient is the analog of the acceleration of gravity. The problem was solved by McLean and Saffman[10] and Vanden-Broeck.[11] A discrete set of solutions was found: for each of these, the shape of the interface is a finger of relative width λ. It was shown subsequently by Kessler and Levine[12] that only the fastest finger is stable against tip-splitting modes. Thus, from the study of the tip re-

gion, one obtains a single stable shape with relative thickness

$$\lambda = f\left[\frac{\Lambda^2 U}{D d_0}\left[c_0(1-K)+\frac{GD}{Um}\right]\right] . \quad (10)$$

Here, f is a decreasing function that has been numerically determined by McLean and Saffman,[10] the properties of which will be discussed in detail in the next section.

Finally, the concentration flux which leaves the tip region is simply

$$-D\frac{dc}{dz} = \lambda\left[c_0(1-K)U + D\frac{G}{m}\right] - D\frac{G}{m} . \quad (11)$$

3. The tail region

At some distance larger than Λ from the tip, the advective term $U\,\partial c/\partial z$, which was negligible in the tip region, cannot be neglected. A new balance occurs between advection and transverse diffusion which leads to the Scheil equation for the shape of the tail in the case of stationary growth (see Hunt[13]). For instance, when the miscibility gap is assumed constant, the shape of the tail is an exponential profile which goes to $y=\pm\Lambda/2$ on a length scale $l_T = |m|c_\infty(1-K)/KG$ determined by the temperature gradient, on the same order of the diffusive length.

The asymptotic matching of this tail to the finger shape of the tip was done by Dombre and Hakim[14] in the limit of $\lambda \approx 1$ and for stationary conditions. The main result is that this matching gives no constraint to the tip-region shape, and that, in particular, the primary spacing of the cells Λ is not determined. This result was confirmed numerically by Ben Amar and Moussalam[15] for other values of λ. An important consequence of these results is that the tail region can be ignored for the determination of the tip-region shape and thus for the determination of the concentration flux released by the cell. We assume that the same property holds in the case of a slow instationary process, on the diffusive time scale.

C. Equations of motion

To summarize, in the small-Peclet-number limit, and under the assumption that the tail region does not affect the tip region, the full free-boundary problem can be reduced to a set of equations of motion for the cell tips, located at the position $z_0(t)$ and moving like point sources in a semi-infinite monodimensional medium. For convenience, we define the dimensionless concentration field $u = K(c-c_\infty)/c_\infty(1-K)$ and introduce the notation $1/2\nu = D/Ul_T$. For $z > z_0$, u satisfies

$$\frac{\partial u}{\partial t} + U\frac{\partial u}{\partial z} = D\frac{\partial_u^2}{\partial z^2} , \quad (12)$$

with the following boundary conditions at $z=z_0$,

$$u = 1 - z_0/l_T , \quad (13)$$

as can be deduced from Eq. (5), and

$$-D\frac{du}{dz} = U\left[\frac{1}{2\nu} + \lambda\left[1-(1-K)\frac{z_0}{l_T} - \frac{1}{2\nu}\right]\right] , \quad (14)$$

as can be deduced from Eq. (11). Here,

$$\lambda = f(C) , \quad (15)$$

where

$$C = \frac{\Lambda^2 U}{D d_0}\left[1-(1-K)\frac{z_0}{l_T} - \frac{1}{2\nu}\right] \quad (16)$$

is the analog of the control parameter in viscous fingering.

III. STEADY-STATE SOLUTIONS

In the preceding section we derived the equations of motion governing the dynamics of cell tips. To obtain the steady-state solutions of this set of equations, we first rewrite Eq. (1) in a frame moving with the interface at velocity U:

$$D\frac{d^2u}{dz^2} + U\frac{du}{dz} = 0 . \quad (17)$$

The steady-state concentration profile which solves Eq. (17) subject to the boundary condition at the interface equation (13) is then simply

$$u(z) = (1-z_0/l_T)\exp[-(U/D)(z-z_0)] . \quad (18)$$

Substituting Eq. (18) into the flux conservation relation (14), we obtain

$$\Delta = \frac{K\lambda + (1-\lambda)/2\nu}{1-(1-K)\lambda} , \quad (19)$$

where we have defined the dimensionless tip undercooling:

$$\Delta = 1 - z_0/l_T . \quad (20)$$

The steady-state solutions of our model are then completely determined by Eq. (19), together with the relation between the finger width λ and the cell spacing Λ contained in Eq. (15), with

$$C = \frac{K(1-1/2\nu)}{1-(1-K)\lambda}\frac{\Lambda^2 U}{d_0 D} , \quad (21)$$

obtained by combining Eqs. (16) and (19).

For a material with an isotropic surface tension the function $\lambda = f(C)$ is a decreasing function of C which approaches asymptotically the value $\frac{1}{2}$ for large values of C and has been calculated numerically by McLean and Saffman.[10] Here we use an interpolation formula for $f(C)$:

$$\lambda = f(C) = \frac{(C-\tilde{C})+\tilde{A}}{2(C-\tilde{C})+\tilde{A}} , \quad (22)$$

with $\tilde{C}=2.87$ and $\tilde{A}=50.8$, which reproduces within a few percent their numerical data for values of λ ranging between 1.0 and 0.6. The numerical value of C that we use was determined by Dombre and Hakim,[14] who ana-

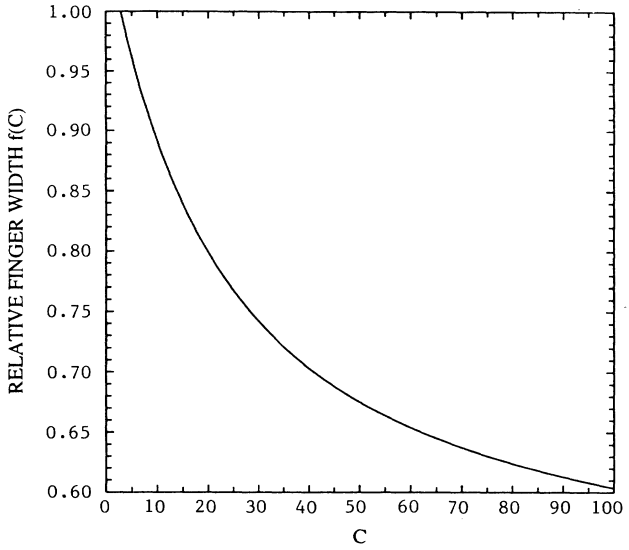

FIG. 2. Numerical interpolation of the curve of McLean and Saffman representing the variations in the finger width λ with the control parameter C.

lyzed the Saffman-Taylor problem in the limit λ close to unity, and it corresponds to the minimum allowed value of C for steady-state shapes. A plot of $f(C)$ is shown in Fig. 2. In Fig. 3 we show a plot of the dimensionless tip undercooling $\Delta(C)$ obtained by combining Eqs. (19) and (22) for three values of ν. Since at fixed velocity U the cell spacing Λ is uniquely determined by the control parameter C via Eq. (21), $\Delta(C)$ represents a one-parameter family of steady-state shapes with varying cell spacing and tip undercooling. Note that the tip undercooling varies very little with Λ for sufficiently large values of Λ (or, equivalently, sufficiently large values of C) and approaches the limiting value

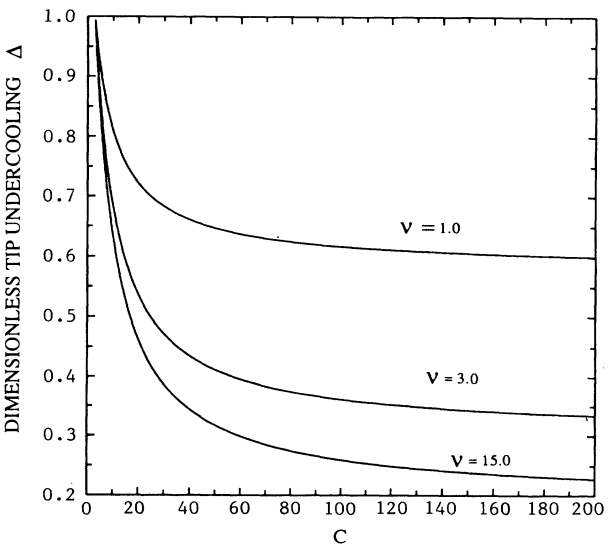

FIG. 3. Variations of the dimensionless tip undercooling Δ with the control parameter C for $K=0.2$ and three values of ν.

$$\tilde{\Delta}=\frac{K(1+1/2\nu)}{1+K} \tag{23}$$

as λ goes to $\frac{1}{2}$. As ν increases, Δ decreases. Both the relative flatness of the curve $\Delta(C)$ at sufficiently large cell spacings and the decrease of Δ with increasing velocity have been observed previously by Hunt and McCartney,[16] who determined numerically the shape of deep cells for small values of the Peclet number. Our analysis is not valid at Peclet numbers of order unity or larger where, as demonstrated numerically by Ungar and Brown,[17] $\Delta(C)$ has a minimum at a finite value of the control parameter C.

Experimentally, the tip undercooling of deep cells has been observed by Esaka and Kurz[18] to decrease with increasing velocity. One needs, in principle, an additional relation to determine uniquely the tip undercooling and compare the predictions of our analysis to experiment. Since at this point such additional relation has not yet been rigorously derived, one can only interpret this last experimental observation to suggest that the selected cell spacing corresponds to a tip undercooling which lies inside the broad flat region of the curve $\Delta(C)$.

In our analysis we have assumed the surface tension to be isotropic. It is, in principle, possible to include the effect of a finite surface-tension anisotropy. For this purpose one would need to repeat the calculation of McLean and Saffman with a finite amount of crystalline anisotropy and determine numerically the corresponding curve $\lambda=f(C)$. Existing theoretical and experimental results suggest that this curve lies below that of McLean and Saffman in Fig. 2. First, the asymptotic behavior of $f(C)$ at finite anisotropy has been investigated analytically by Dorsey and Martin,[19] who demonstrated that $f(C)$ approaches asymptotically zero for large values of the control parameter C. Secondly, the experiment of Bechhoefer, Guido, and Libchaber[20] on crystal growth in a capillary tube has shown that, for nearly identical growth velocities, the finger width of a pivalic acid crystal (anisotropic material) is smaller than that of a succinonitrile crystal (more isotropic material).

IV. OSCILLATORY INSTABILITY

A. Linear-stability analysis

To derive the eigenvalue equation we linearize the equations of motion (12)–(16) around the steady-state solutions defined by Eqs. (18)–(20) and restrict our attention to perturbations of the form

$$\delta u = A \exp[\omega t + k(z - z_0)], \quad \mathrm{Re}(k) < 0 \tag{24}$$

and

$$\delta z_0 = B \exp(\omega t) . \tag{25}$$

We shall find that for some values of the control parameters the real part of ω becomes positive with a finite imaginary part, this corresponding to an oscillatory instability of the cell tips.

Substituting Eq. (24) in Eq. (12), one obtains

$$Dk^2 + Uk - \omega = 0 . \tag{26}$$

We restrict our attention to the mode with a positive real part. Since $\mathrm{Re}k<0$, the allowed solution is

$$k=-(U/2D)\{1+[1+4(\omega D/U^2)]^{1/2}\}\ , \tag{27}$$

where, by convention, the square root has a positive real part.

Then, substituting Eqs. (24) and (25) in Eqs. (13) and (14), one obtains, respectively, the following relations between A and B:

$$A-B\frac{U}{D}\left[1-\frac{z_0}{l_T}\right]=-\frac{B}{l_T} \tag{28}$$

and

$$-D\left[Ak+B\left[\frac{U}{D}\right]^2\left[1-\frac{z_0}{l_T}\right]\right]=B\left[\left[\frac{d}{dU}(\lambda U)\omega+U\frac{d\lambda}{dz_0}\right]\left[1-(1-K)\frac{z_0}{l_T}\right]-\frac{D}{l_T}\left[\frac{d\lambda}{dU}\omega+\frac{d\lambda}{dz_0}\right]-\frac{\lambda U}{l_T}(1-K)\right]\ . \tag{29}$$

By eliminating A and B between these two relations, one obtains the following eigenvalue equation for the dimensionless growth rate $\Omega=\omega 2D/U^2$:

$$(\Delta-1/2v)\sqrt{1+2\Omega}=a\Omega+b\ , \tag{30}$$

or

$$a^2\Omega^2+2[ab-(\Delta-1/2v)^2]\Omega+b^2-(\Delta-1/2v)^2=0\ , \tag{31}$$

with the condition that the right-hand side of Eq. (30) has a positive real part. Here, a and b are two quantities depending on the steady-state shapes:

$$a=\left[1-(1-K)\frac{z_0}{l_T}\right]\frac{d}{dC}[Cf(C)] \tag{32}$$

and

$$b=\Delta+\frac{1}{2v}-\frac{1-K}{v}\frac{d}{dC}[Cf(C)]\ . \tag{33}$$

It is convenient to express these quantties as a function of the relative finger width λ using the steady-state relation (19). The expressions for a a and b become

$$a=\frac{K+(1/2v)(1-K)(1-\lambda)}{1-\lambda(1-K)}\frac{d}{dC}[Cf(C)]\ , \tag{34}$$

$$b=\frac{(1-\lambda)/v+K\lambda(1+1/2v)}{1-\lambda(1-K)}-\frac{1-K}{v}\frac{d}{dC}[Cf(C)]\ , \tag{35}$$

and

$$\Delta-\frac{1}{2v}=\frac{K\lambda(1-1/2v)}{1-\lambda(1-K)}\ . \tag{36}$$

B. Limiting case

The physical origin of the oscillatory instability can be understood more clearly by examining two important limiting cases of the eigenvalue equation (31).

1. The planar interface

This limit is formally obtained when $\lambda=1$, and $df/dC=0$. The growth-rate equation can be written as

$$\Omega^2+2\frac{\Omega}{v}\left[\frac{1}{2}+K-\frac{1}{4v}\right]+\frac{K}{v}\left[2-\frac{1}{v}+\frac{K}{v}\right]=0\ . \tag{37}$$

When $1/8v<K<1$, Ω has a nonzero imaginary part and a negative real part equal to

$$\mathrm{Re}\Omega=-(1/2v)(1+2K-1/2v)\ . \tag{38}$$

When $1/v$ is small, the growth rate is simply

$$\Omega=-(1/v)(1+2K)\pm i\sqrt{2K/v}\ . \tag{39}$$

Thus, in this limit, the interface motion undergoes damped oscillations. The physical origin of the damping can be explained as follows. First, consider a perturbation where the interface is slightly displaced towards the high-temperature region. The effective undercooling slightly decreases and the released concentration flux is reduced. As a result, the interface velocity decreases and the interface comes back to the low-temperature region.

2. Crystal growth in a capillary tube

When there is no temperature gradient ($1/v=0$), the system is equivalent to the growth of a crystal in a capillary tube. The crystal is assimilated to one of the cells of the array and the distance between the walls to the primary spacing Λ. In this limit, the eigenvalue equation reduces to a form derived previously by Pelcé.[21] It has a nonzero solution equal to

$$\Omega=-\frac{Cf(C)\dfrac{df(C)}{dC}}{\left[\dfrac{d}{dC}Cf(C)\right]^2}\ . \tag{40}$$

Since $f(C)$ is a decreasing function of C, the growth rate is real and positive and leads to an instability of the stationary cell. To understand this effect, consider a perturbation which increases slightly the relative finger width. More solute will be rejected and the effective undercooling will be reduced. As a result, the crystal will slow down and become even thicker, since a slower motion corresponds to a larger relative width. Note that the strength of the instability (the magnitude of Ω) is proportional to the quantity $C\,df(C)/dC$ plotted in Fig. 4.

When both effects are considered, as is the case in the

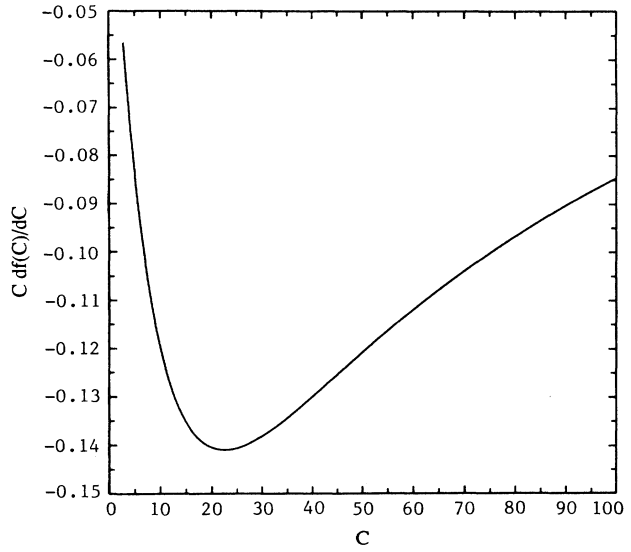

FIG. 4. Plot of $Cdf(C)/dC$ vs C, where $f(C)$ corresponds to Fig. 1.

complete growth-rate equation, one expects that for some values of the control parameter an oscillatory instability will appear. Consider a sufficiently large value of $1/\nu$, i.e., a strong temperature gradient. The first effect (planar interface) will dominate and the interface will be damped in an oscillatory way. If the temperature gradient is decreased, the second effect (crystal in the capillary tube) will appear and the real part of the growth rate will become positive, still with a finite imaginary part. The competition between these two effects will therefore lead to an oscillatory instability. As mentioned previously, the strength of the instability is related to the value of $C\,df(C)/dC$, which has a maximum in absolute value for some finite value of C (see Fig. 4). Thus it is expected that the oscillatory instability appears first for a finite nonzero value of C. How the system evolves after onset of this instability cannot be answered in the context of the linear analysis performed here. However, a nonlinear analysis of the equations of motion (12)–(16) could, in principle, be performed to determine the nature of the Hopf bifurcation (subcritical, supercritical) and to predict the evolution of the system above threshold of the instability.

C. Numerical results and stability limit

Assume that surface tension is isotropic, then $f(C)$ is the McLean-Saffman curve. We have drawn in Fig. 5 the real and imaginary parts of the growth rate Ω determined numerically for $K=0.2$ and three values of $1/\nu$. For small $1/\nu$ there is a large range of unstable states, with a nonzero imaginary part, between two extreme values $C_{\min}$ and $C_{\max}$ (i.e., $\mathrm{Re}\Omega>0$ for $C_{\min}<C<C_{\max}$) that can be determined analytically. For large $1/\nu$ all steady states are stable. For an intermediate $1/\nu_c$ only one state, C_c, becomes unstable. We draw in Fig. 6 the stability limits $1/\nu_c(K)$ and the corresponding values of $C_c(K)$.

For large values of $1/\nu$, one can derive analytically the stability limits $C_{\min}$ and $C_{\max}$ for the oscillatory instability. In both cases the important term giving the instability, $C\,df(C)/dC$, is small and can balance the small stabilizing factor $1/\nu$.

When C is close to C (defined in Sec. III), λ is close to 1 and the growth-rate equation can be approximated by

$$\Omega^2+2\frac{\Omega}{\nu}\left[\tfrac{1}{2}+K+\nu C\frac{df}{dC}\right]+2\frac{K}{\nu}=0\ . \tag{41}$$

The stability threshold is obtained for $\mathrm{Re}\Omega=0$, i.e., for $C=C_{\min}$, where

$$C_{\min}\frac{df}{dC}(C_{\min})=-\frac{1}{\nu}(K+\tfrac{1}{2})\ . \tag{42}$$

At the instability threshold, Ω has a nonzero imaginary

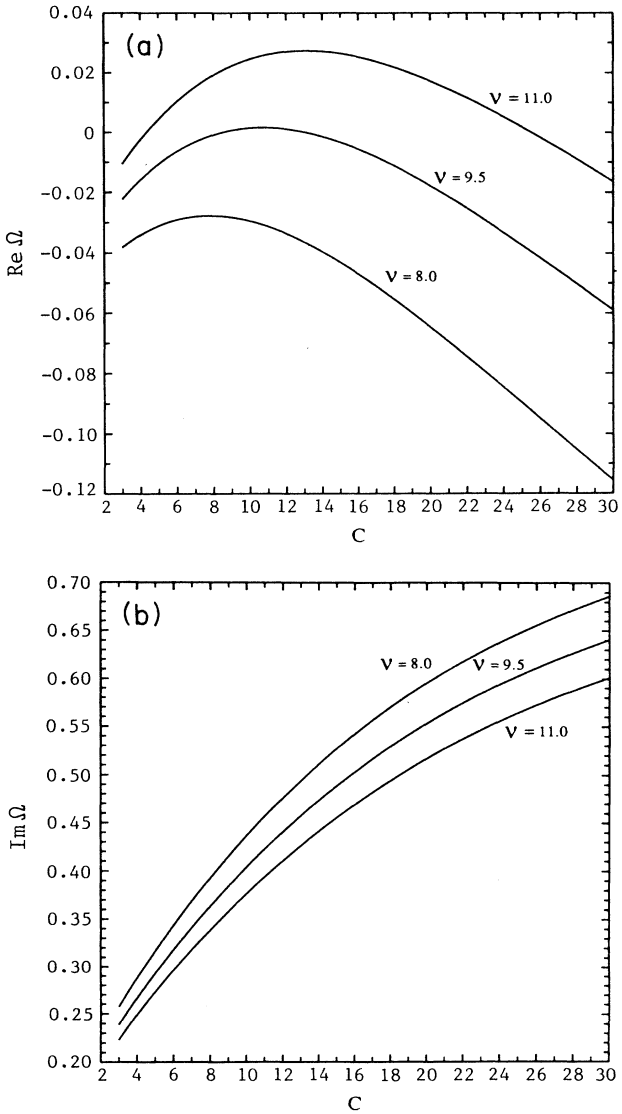

FIG. 5. Oscillatory instability: (a) real part of Ω vs C, and (b) imaginary part of Ω vs C for $K=0.2$ and three values of ν. Here the instability first appears at $\nu_c=9.5$ and $C_c=11$.

part equal to $(2K/v)^{1/2}$.

When C is large, λ is close to $\frac{1}{2}$ and the growth-rate equation can be approximated by

$$\Omega^2+2\frac{\Omega}{v}\left[\frac{3}{4K}+\frac{5}{4}+\frac{K}{2}+2vC\frac{df}{dC}\right]+\frac{1}{Kv}(1+K)^2=0 . \tag{43}$$

At the threshold, the term proportional to Ω vanishes, and one obtains

$$C_{\max}\frac{df}{dC}(C_{\max})=-\frac{1}{2v}\left[\frac{K}{2}+\frac{5}{4}+\frac{3}{4K}\right] . \tag{44}$$

The corresponding imaginary part of the growth rate is,

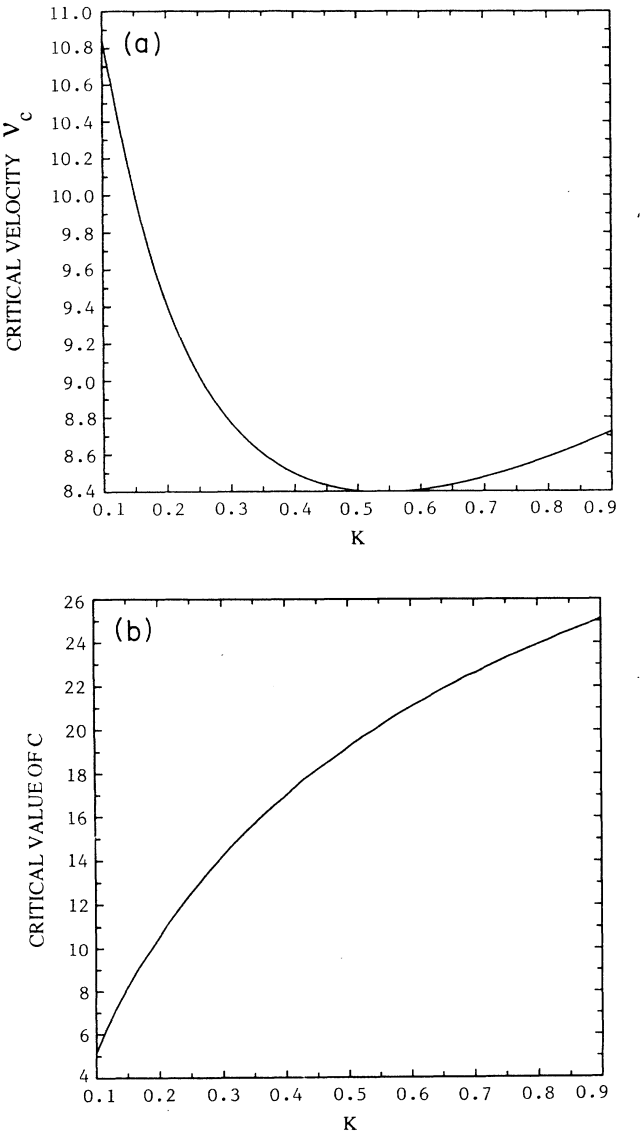

FIG. 6. (a) Stability limits for the oscillatory mode. The area above the solid curve is unstable and the one below is stable. (b) Variations of the critical value of C at threshold of the oscillatory instability (C_c) with K.

at this point,

$$\mathrm{Im}\Omega=\frac{1+K}{\sqrt{Kv}} . \tag{45}$$

Let us now discuss the effect of an anisotropy in the surface tension. This effect appears only via the function $f(C)$ and thus will only influence the strength of the instability via the factor $C\,df(C)/dC$. As mentioned in the preceding section, several observations indicate that the anisotropy factor lowers the value of $f(C)$ for a given nonzero value of C. This leads to steeper variations of $f(C)$ and thus larger values of $C\,df(C)/dC$. Thus one can expect that, for a given temperature gradient, the oscillatory instability should appear at a lower critical velocity for a more anisotropic material.

In performing a linear-stability analysis of Eqs. (12)–(16), we have assumed that the interfacial front is periodic of period Λ. Without this constraint other linear modes and, in particular, long-wavelength modes could also, in principle, become unstable and supress the oscillatory instability. The competition of nearby tips which is known to cause an instability in the Saffman-Taylor system undoubtedly plays an important role in directional solidification in the small-Peclet-number limit. This problem appears beyond the scope of the paper. For the moment, one can expect that even if the oscillatory instability is wiped out at small Peclet number by a spatiotemporal instability, it plays an important role for Peclet number of order 1, for which the tip competition becomes less effective.

V. DISCUSSION

In this paper we have analyzed in the small-Peclet-number limit the linear stability of deep cells against perturbations which displace their tip position z_0, and have found that such a perturbation will grow in an oscillatory way when the velocity of the solidification front exceeds a threshold value determined by $v_c(K)$. The relative cell width λ is directly related to z_0 and oscillates in phase with the tip position. For velocities increasingly larger than the threshold velocity, an increasingly larger range of cell spacings becomes unstable.

This new instability limits the parameter range for which steady-state microsegregation can occur and is therefore of considerable importance for our understanding of microstructures.

The physical origin of this oscillatory instability clearly appears to come from the interaction of the cell-tip motion with the boundary layer of solute ahead of the interface. In particular, two competing effects result from this interaction: a stabilizing effect due to the temperature gradient and a destabilizing effect due to the variability of the relative cell width λ.

The experiments of Eshelman *et al.*[6] in directional solidification of pivalic acid show the apparition of coherent sidebranching for a critical $v\approx 7$, the corresponding Peclet number being $P\approx 1$. The sidebranching wavelength seems to scale with the tip region. Our analysis deals with the small-Peclet-number limit and we find that the frequency of the sidebranching $\Omega\approx U/\Lambda$

scales like P. We think that we have isolated the oscillatory mode which, if extrapolated to Peclet numbers of order unity, is responsible for the coherent sidebranching observed experimentally. At this point, there is a need for numerical studies to confirm that the extension to Peclet numbers of order unity is regular.

ACKNOWLEDGMENTS

One of us (A.K.) wishes to thank the California Institute of Technology and the Weingart Fellowship Program for its financial support, and the hospitality of the Laboratoire de Recherche en Combustion at l'Université de Provence.

[1]A. Dougherty, P. D. Kaplan, and J. P. Gollub, Phys. Rev. Lett. **58**, 1652 (1987).
[2]R. Pieters and J. S. Langer, Phys. Rev. Lett. **56**, 1948 (1986).
[3]M. Barber, A. Barbieri, and J. S. Langer, Phys. Rev. A **36**, 3340 (1987).
[4]J. S. Langer, Phys. Rev. A **36**, 3350 (1987).
[5]P. Pelcé and P. Clavin, Europhys. Lett. **3**, 907 (1987).
[6]M. A. Eshelman, V. Seetharaman, and R. Trivedi, Acta Metall. **36**, 1165 (1988).
[7]J. S. Langer, Rev. Mod. Phys. **52**, 1 (1980).
[8]P. Pelcé and A. Pumir, J. Cryst. Growth **73**, 337 (1985).
[9]A. Karma, Phys. Rev. A **34**, 4353 (1986).
[10]J. W. McLean and P. G. Saffman, J. Fluid Mech. **102**, 445 (1981).
[11]J. M. Vanden-Broeck, Phys. Fluids **26**, 2033 (1983).
[12]D. Kessler and H. Levine, Phys. Rev. Lett. **57**, 3069 (1986).
[13]J. D. Hunt, in *Solidification and Casting of Metals* (The Metals Society, London, 1979), Bks. 192 and 193.
[14]T. Dombre and V. Hakim, Phys. Rev. A **36**, 2811 (1987).
[15]M. Ben Amar and B. Moussallam, Phys. Rev. Lett. **60**, 317 (1988).
[16]J. D. Hunt and D. G. McCartney, Acta Metall. **35**, 89 (1987).
[17]L. H. Ungar and R. A. Brown, Phys. Rev. B **31**, 5931 (1985).
[18]H. Esaka and W. Kurz, J. Cryst. Growth **72**, 578 (1985).
[19]A. T. Dorsey and O. Martin, Phys. Rev. A **35**, 3989 (1987).
[20]J. Bechhoefer, H. Guido, and A. Libchaber, C. R. Acad. Sci. Paris **306**, Serie II, 619 (1988).
[21]P. Pelcé, Europhys. Lett. **7**, 453 (1988).